Research Journal of Chemical Sciences ISSN 2231-606X
Vol. **16(1),** 63-73, February **(2026)** *Res. J. Chem. Sci.*

Design and Investigations of Fluconazole Nanoparticles Doped Poly (vinyl alcohol) Composite Films for Food Packaging Uses

Shwetarani Rajamani[1], Ramesh Sabu Gani[1*], Deepak Ramesh Kasai[2], Nivedita Rajashekhar Bashetti[3], Govinda Anjanayya[4], Avinash Arasidaa Kamble[4], Ravindra Basappa Chougale[5] Saraswati Purandar Masti[6]

[1]Department of Industrial Chemistry, Mangalore University, Mangalagangothri, Mangalore-574199,State, Karnataka, India
[2]Department of Chemistry, KLEs S. Nijalingappa College, Rajajinagar, 2nd Block Bangalore 560010, State Karnataka, India
[3]Department of Studies in Biotechnology and Microbiology, Karnataka University, Dharwad-580003.State, Karnataka, India
[4]Department of Industrial Chemistry, Mangalore University, Mangalagangotri, Mangalore-574199,State, Karnataka, India
[5]Department of Chemistry, Karnataka University, Dharwad-580003.State, Karnataka, India
[6]Department of Chemistry, Karnataka Science College, Dharwad - 580001. State, Karnataka, India
ramesh180769@gmail.com

Available online at: www.isca.in, www.isca.me
Received 14th December 2025, revised 25th January 2026 accepted 9th February 2026

Abstract

Integrating functional agents into food packaging can prolong the serviceable life of products while preserving their standard and condition, also enhancing their attractiveness. The polyvinyl alcohol (PFLNPs) composite films that were used in the synthesis of fluconazole nanoparticles (PFLNPs) were produced by the solvent casting technique. The produced PVA and PFLNP composite films were characterized to examine morphology, mechanical properties, hydrophilicity, and antimicrobial characteristics utilizing UV, FT-IR, XRD, SEM, UTM, WCA, and antimicrobial assays. The study's findings indicated that the consistent integration of PFLNPs into the PVA matrix for food packaging applications resulted in improved crystallinity, enhanced intermolecular interactions, mechanical properties (Ts increased from 28.25 to 69.04, Ym from 16.21 to 3719 MPa, and a decrease in %Eb from 187 to 6.70), reduced hydrophilicity (from 62.82° to 76.58°), and a smooth, homogeneous morphology. The findings from the XRD analysis indicated a rise in crystallinity corresponding to the increased concentration of PFLNPs. The antimicrobial analysis revealed encouraging antimicrobial activities in opposition to both Gram-positive and Gram-negative bacteria. The findings of this study indicated that the composite films composed of the specified PFLNPs exhibited improved mechanical and antibacterial properties, potentially benefiting the pharmaceutical and food sectors.

Keywords: PVA, fluconazole, mechanical, morphology, antimicrobial and food packaging.

Introduction

In recent decades, pollution from non-biodegradable and fossil fuel-derived plastics has escalated. The escalating menace of climate change, pollution, and the exhaustion of fossil fuels is driving a transition from disposable polymers sourced from fossil fuels to biodegradable polymers[1-3]. A significant environmental hazard is the extensive utilisation of petrochemical packaging for food preservation, which is neither biodegradable nor renewable. In response to the issues presented by non-degradable plastic waste, several efforts have been undertaken[4]. It is thus necessary for the food packaging industry to have a material that is non-toxic, conveniently available, cost-effective, and biodegradable. It is vital to have food packaging in order to preserve the original flavor and texture of the food while it is being stored and transported, as well as to avoid contamination and spoilage. It also provides merchants and consumers with information on the food's manufacturer, storage conditions, expiry date, chemical composition, and more[5].Given that the population of the world reached 8 billion in November 2022 and is continuously expanding, it is impossible to overestimate the significance of having a food supply that is nutritious[6]. Additionally, it is crucial to increase product sales through the use of visually appealing patterns and colours. The creation of new active packaging solutions that are manufactured from naturally occurring active compounds has been a part of the process of developing new food packaging. This novel packaging solution was developed with the twin objectives of prolonging the shelf life of the food that is packed and making the product more ecologically friendly[7]. Both of these objectives were taken into consideration throughout the design process. The term "biodegradable" denotes substances that can be decomposed by naturally occurring microorganisms. These microbes generate an organic by-product while not emitting any harmful gases. Biodegradable and antimicrobial polymeric films have garnered a significant amount of interest in the packaging industry. This is mostly attributable to the growing environmental concerns and problems related with plastic waste in the last several decades, which have been propelled by a strong commitment to improving living conditions all over the world[8].It is necessary for the materials used for packaging to be created entirely from renewable biopolymers, such as polyvinyl alcohol (PVA),

starch, chitosan, cellulose, and natural gums, in order for them to be considered biodegradable. These materials should break down into their natural components upon disposal, ensuring that no toxic gases are released in the process[9]. A ground breaking, eco-conscious material must possess adequate durability. The objective is to maintain food freshness by minimizing the presence of microbes that could compromise its quality[10]. One of the characteristics of the synthetic polymer known as poly(vinyl alcohol) is that it is non-toxic, biocompatible, and water-soluble. PVA's hydrophilic properties and excellent film-forming abilities have led to its extensive application in combination with various synthetic and natural polymers[11, 12]. Due to the presence of the hydroxyl (-OH) group in each restating unit of its foundation, a wide range of chemical substances may interact with poly(vinyl alcohol) polymer to result in the formation of a composite film that can accommodate a wide range of packaging requirements and specifications[13,14]. The propensity of composite films to draw moisture, which creates circumstances that are favorable for the development of microorganisms, is one of the primary reasons why the food packaging industry faces substantial and important issues using composite films.

A cross-linking agent or nanoparticles incorporated into the composite film should effectively mitigate PVA's hydrophilicity while enhancing the film's antimicrobial properties[15]. In the past decade, the utilization of nonmaterials has surged across various industries, opening avenues for their prospective application as packaging materials[16].

Materials used for packaging that have been improved by nanotechnology may function in two different ways. By continuously dispensing nano-fillers within the range or limits of a polymer matrix, the interfacial area between the matrix and the fillers is amplified. This, in turn, leads to an increase in the barrier properties, thermal properties, mechanical properties, and characterisation characteristics of the matrix, which eventually results in improved packing outcomes[17,18]. The second way involves the employment of nano-fillers, which allows for the enhancement of food preservation via the use of active packaging. Interactions between the fillers and the packaged food or its surroundings occur very immediately. In the event that nanoparticles are utilized as fillers in the composite film, there is a likelihood that the mechanical and barrier properties of the film may be enhanced[19]. The large surface area, which promotes reactivity, may prevent certain microorganisms from growing on nanoparticles. Antibacterial and biocompatible fluconazole nanoparticles are a potential composite film nano-filler. Nano-fillers in cross linking agents may create a biocompatible, mechanically stable composite film with increased antibacterial characteristics. Fluconazole is an azole antifungal synthetic triazole.The triazole family of solid antifungals includes fluconazole, which inhibits 14-alpha sterol demethylase. This enzyme removes lanosterol from the 14 alpha methyl groups, converting it to ergosterol. Fluconazole reduces fungal ergosterol synthesis and cell membrane function[20]. Adding fluconazole nanoparticles to polymeric nanocomposite food packaging provides antibacterial characteristics. PVA composite films with fluconazole nanoparticles for food packaging are being tested in this project. The effect of nanoparticles in PVA composite film is explored. The nanocomposite films' morphological, thermal, and mechanical characteristics were examined. In manufacturing and using PVA composite sheets for food packaging, antibacterial activity was tested.

Materials and Methods

Fluconazole Nanoparticle Preparation Procedure: PFLNPs were produced by emulsification solvent evaporation and sonication in this investigation[33-35]. Mix 4.81 g Fluconazole and 2.7 g corn starch in a 100-mL beaker, then add 30 mL acetone. Thoroughly stir the mixture and reaction mass at room temperature for 1–2 hours. Dissolve 0.5 g PVA in 100 mL distilled water to make a 0.5% w/v solution in a separate beaker. Before allowing the reaction mixture to sit at room temperature for one to two hours, properly mix and agitate it. Fluconazole solution and polyvinyl alcohol (PVA) solution with a weight-to-volume ratio of 0.5% are combined while being gently swirled.Mix thoroughly and stir at room temperature for 1-2 hours for a homogenous solution. Stir the mixture for another hour to achieve homogeneity. Sonicate the mixture to create an emulsion. Sonication enhances solution constituent dispersion. Allow the emulsified solution to settle for solvent evaporation. This step is crucial to nano hydrogel formation. Evaporation produces nanoparticles from these nanodroplets.

Preparation of PVA-FLZ nano composite film: We prepared nanocomposites by adding 2 g of polyvinyl chloride to a 250 mL beaker containing double distilled water. The whole reaction mass was stirred at room temperature for 24 hours at 35- 40°C until we achieved a clear solution. We took FLZ nanoparticles of different concentrations and sonicated them for 30-45 minutes at 20°C in four different test tubes using 2mL distilled water in each test tube. The nanoparticle solution has been added dropwise by using a syringe at a concentration of 5 mg, 10 mg, 15 mg, and 20 mg to the previously prepared PVA solution, and the solution has been stirred for 3–5 hours than it becomes slightly jell type of colourless solution. Finally, After placing the solution on a Petri dish, we dried it at a temperature of 80°C.

Characterizations: UV-visible spectroscopy: By using a two-beam T80 UV-Vis spectrophotometer that was capable of recording spectra spanning from 200 to 800 nm, we were able to confirm that the PFLNP preparation was correct.

Fourier transforms infrared spectroscopy: Total reflection attenuated PFLNPs and nanocomposite films were tested using Fourier transform infrared (FT-IR) spectroscopy (Prestige 21, Shimadzu, Japan). Measurements were taken at a resolution of 4 cm^{-1} over the 400-4000 cm^{-1} range.

Table-1: Composition table of FLZ nanoparticles doped PVA composite films.

Sample code	PVA (g)	PVA/FLZ nanoparticles (g)
PVA	2	00
PFLNPs-1	2	0.005
PFLNPs-2	2	0.010
PFLNPs-3	2	0.015
PFLNPs-4	2	0.020

X-ray diffraction: Ragaku D/Max-IIA X-ray diffraction, which is located in Tokyo, Japan, was used by the researchers in order to investigate the production of FLNPs, the influence of crystallinity on PVA composite films, and the impact of crystallinity on PFLNPs.A Cu-Ka source running at 30 kV (with a wavelength of 51.5410 degrees) was responsible for the radiation. We scanned the samples at a rate of 28 per minute, using a current of 20 mA from 0° to 80°. We used the diffracted intensity data to determine the crystallinity. We used Scherer's equation (1) to extract "P" from the noticed WAXD data for evaluating the usual crystallite sizes.

$$P = \frac{k\lambda}{\beta cos\theta} \quad (1)$$

The structure of the crystal, the Miller index of reflecting crystallographic planes, and the morphology of the crystallites all have a role in determining the value of the constant k=0.9. The symbol θ is used to denote the Bragg angle, while the symbol λ=1.5406 Å conveys the wavelength of the X-ray photon. In radians, the symbol β denotes the breadth of the reflection when the intensity is decreased by half.

Scanning electron microscopy: Through the use of JEOL JSM-6360 scanning electron microscopy, we investigated the morphology of FLNP and PFLNP composite films as well as their production processes. Experiments were carried out at an acceleration of 10 kV. All of the test pieces were sputtered coated with conductive gold prior to the beginning of the experiment in order to lessen the impact of the powerful electron beams during the charging process. Through the use of double-sided carbon tape, film specimens were affixed to the sample container.

Mechanical studies: LLOYD Instrument's universal testing machine (UTM) assessed mechanical properties. TS, Eb, and Ym were measured using ASTM D882-91 standards. Extension grips on the testing equipment were used to securely hold the rectangular film samples that measured 2.5 centimeters by 10 centimeters. In a temperature-controlled environment, the system processed film samples at a rate of 5 millimeters per minute.

Water contact angle measurement: We measured composite film contact angles to determine hydrophilicity and hydrophobicity. SEO Phoenix measured water contact angle. All investigations used a seven µL drop volume at ambient temperature. We used the right software to measure contact angles at five places.

Antimicrobial studies: The antibacterial efficacy was evaluated via Muller-Hinton agar. Polymer solutions were prepared at a concentration of 50 mg/mL. The organisms examined included Staphylococcus aureus, Bacillus cereus, Escherichia coli, and Pseudomonas aeruginosa.The medium was poured onto sterile petri dishes. The solidification test was followed by organism injection. Use a cork borer to form eight milliliter wells, then fill with 50 µL of film solution. A 1 mg/ml Streptomycin solution was the positive control. Plates were incubated at 37°C for 24 hours. We checked the plates for an inhibiting zone around the wells. Results were based on the inhibitory zone's mean millimeter diameter. The results of the triple experiment are shown as mean ± SD.

Results and Discussion

UV-Visible spectroscopy: PFLNP UV spectra are shown in Fig.1. UV-Vis spectroscopy confirmed PFLNP production. Each element has a specified quantity of free electrons, causing an absorption peak. Nanoparticle size and shape determine this peak's location. The peaks at 374 nm in Figure-1 demonstrate PFLNP production.

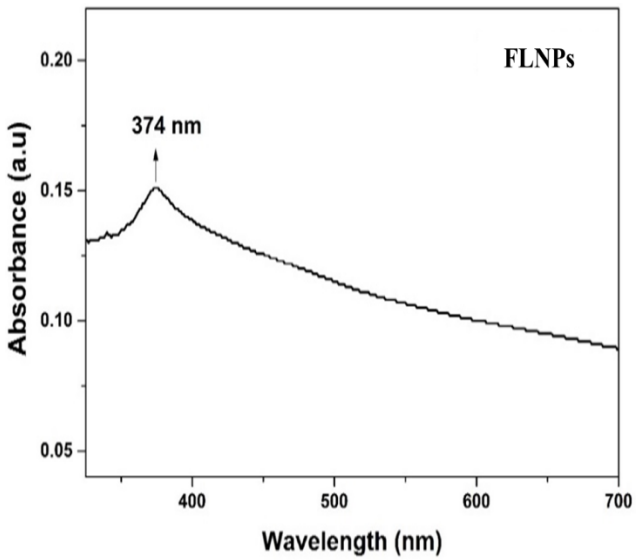

Figure-1: UV spectra of PFLNPs.

Fourier transforms infrared spectroscopy: Figure-2 shows pure PVA, PFLNPs, and composite film FT-IR spectra. In Figure-2, pure PVA displayed peaks at 3309, 2932, 1717, 1433, 1368, 1258, 1092, and 844 cm-1 for hydroxyl (O–H), -CH2, C=O, C–H, CH2 (bending vibration), C–H (vibrational bands), C–H (wagging), C–O (acetyl group stretching), and C–C21, 22.

Fluconazole nanoparticles also demonstrated a large vibration range from 3300 to 3600 cm-1 due to hydrogen-bonded –OH stretching. These bands were the aromatic ring's C=C stretching and the triazole ring's stretching peak at 1644 and 1433 cm-1. The C-F group peaks at 1258 cm-1 and the C-H aromatic ring at 1010 cm-1. Peaks were 912 and 844 cm-1 23, 24. PVA and fluconazole nanoparticle hydrogen bonding interactions cause PFLNPs composite films to have a smaller –OH stretching peak position than PVA films. Peak change shows effective intercalation, creating a uniform nanocomposite layer. The spectra of PVA film with PFLNPs did not change, perhaps owing to overlapping peaks.

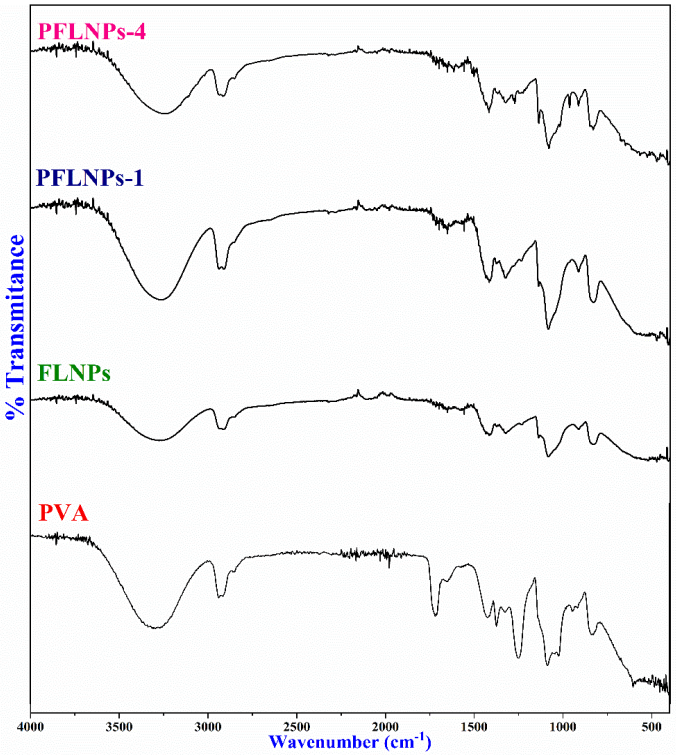

Figure-2: FTIR spectra of PVA and PFNLPs composite films.

X-ray diffraction: X-ray diffraction (XRD) studies have exhibited valuable insights into the crystalline and amorphous compositions of the material. The XRD patterns for both pure PVA and the FLNPs doped PVA composite films are presented in Figure-3. In Figure-3, a pronounced peak is noticed at 2θ-19.41, which is linked to the broad amorphous peak connected with the combination of the 101 and 101 planes. Attia G et al. have documented a comparable finding[25]**.** The crystallinity and amorphous phases related to semi-crystalline polymers are identified by the presence of sharp peaks alongside dispersed scattering, as is well established in the literature [26, 27]**.** Strong intermolecular interactions among PVA chains, The creation of the crystalline phase of polyvinyl alcohol (PVA) was caused by the presence of hydrogen bonds that are connected to a monoclinic unit cell that has already previously established. In contrast to the strong diffraction peaks that were found in other locations, the composite films that were made up of the four PFLNPs had a peak that was somewhat wide and fell within the range of 2 = 22.63 to 23.06.One possible explanation for the diffraction patterns seen in PFLNPs nanocomposite films is that these patterns are caused by a little amount of crystallinity in conjunction with a considerable quantity of diffuse scattering. This suggests that there is a minor nanocrystalline phase of PVA present in addition to the amorphous phase that is typically seen in the bulk. After doing a more in-depth analysis of the diffraction profiles, it was shown that the sharpness of the diffraction peak continually improves as the concentration of PFLNPs increases.

Scanning electron microscopy (SEM) and Energy-Dispersive X-ray Spectroscopy (EDX): Scanning electron microscopy (SEM) and Energy-Dispersive X-ray Spectroscopy (EDX) Fluconazole.

Figure-4a represents the SEM images of the pure fluconazole (FL). It is evident from the Fig.4a that fluconazole is almost irregular agglomerated spherical like homogeneous and slightly crystalline in nature. Smooth, elongated or plate-like shapes were the particles' outward manifestations. A well-defined structure, as shown by the crystalline character, may impact solubility and bioavailability. The homogeneity of the particles confirms the presence of FL highlighting the significance of the FL in various activities determined for food packaging applications. In Figure-4a, EDX spectra confirms the presence of C, O, F, Pd, and Au. The elemental analysis confirms that uniform formation of fluconazole and no significant impurities were detected confirming the purity of the synthesized nanoparticles. There is a chance that the weak Au and Pd line that was seen in the spectrum is the result of the gold coating that was put to the surface of the sample. This suggestion is supported by other evidence.Fig.4b represents the SEM and EDX images of the fluconazole nanoparticles (PFLNPs). SEM images in the Fig.4b depicted that fluconazole nanoparticles as regular elongated rod like structures indicating possible crystalline in nature. Smooth, elongated or plate-like shapes were the particles' outward manifestations. Elements C, N, O, and F are present in the stoichiometric ratio as shown in Fig.4b, as revealed by the energy-dispersive X-ray spectra.

The morphology of PVA and the presence of PFLNPs within the PVA matrix were analyzed through SEM techniques. Figure-5 displays SEM micrographs of pure PVA, PFLNPs-1, and PFLNPs-3. The prepared virgin PVA film exhibits a smooth and homogeneous morphology[28, 29]**.** The SEM micrographs of PFLNPs nanocomposite films exhibited uniformity and regular dispersion of FLNPs within the PVA matrix (PFLNPs-1 and PFLNPs-3). This discovery may be due to the hydrogen bonding that occurs throughout the multicomponent system, with PVA acting as the holding matrix[30]**.**Figure 5 provides a good illustration of the presence of nano-sized particles inside the PVA polymer film. These particles are uniformly dispersed throughout the PVA structure since they are nano-sized.

According to the data shown in Figure 5, the modification of the PVA film that included PFLNPs led to the dispersion of circular particles throughout the PVA film. It has been hypothesized that the structures that are the product of substantial interactions between PVA and PFLNPs are white circular-shaped particles that range in size.

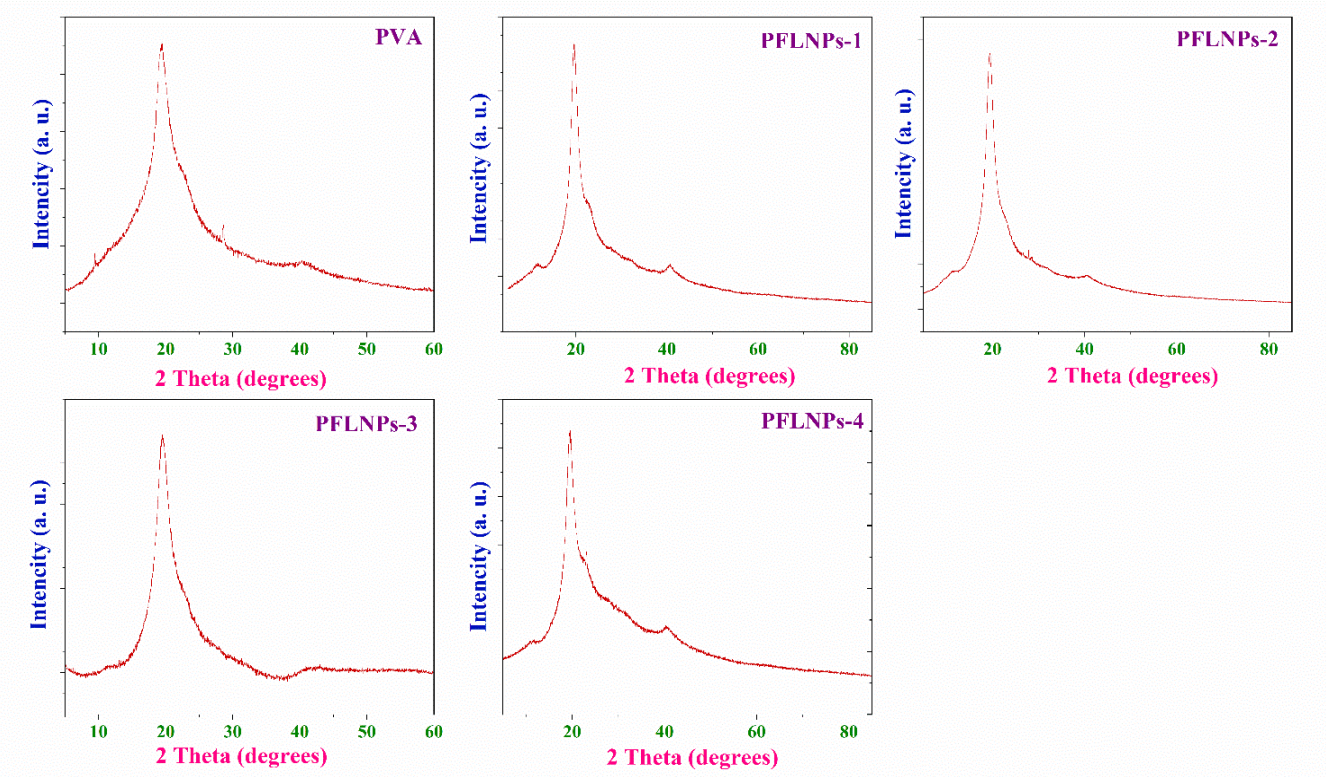

Figure-3: X-ray diffraction images of PVA and PFLNPs composite films.

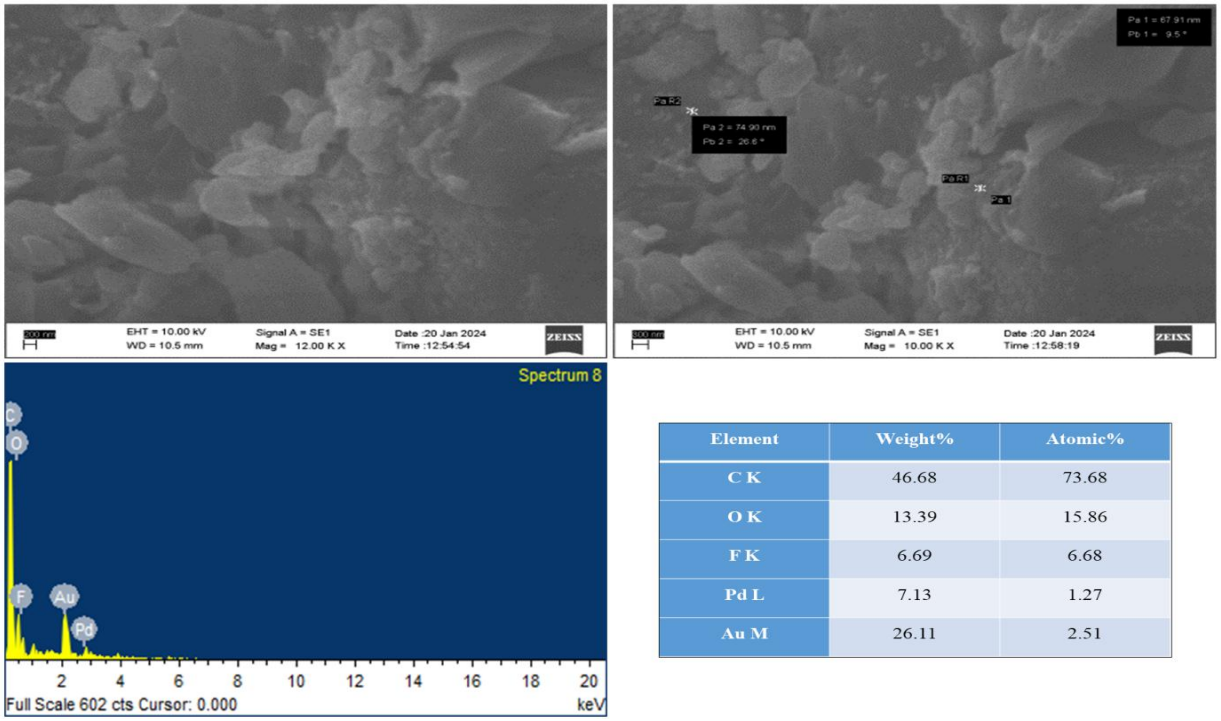

Element	Weight%	Atomic%
C K	46.68	73.68
O K	13.39	15.86
F K	6.69	6.68
Pd L	7.13	1.27
Au M	26.11	2.51

Figure-4a: SEM and EDX images of pure Fluconazole.

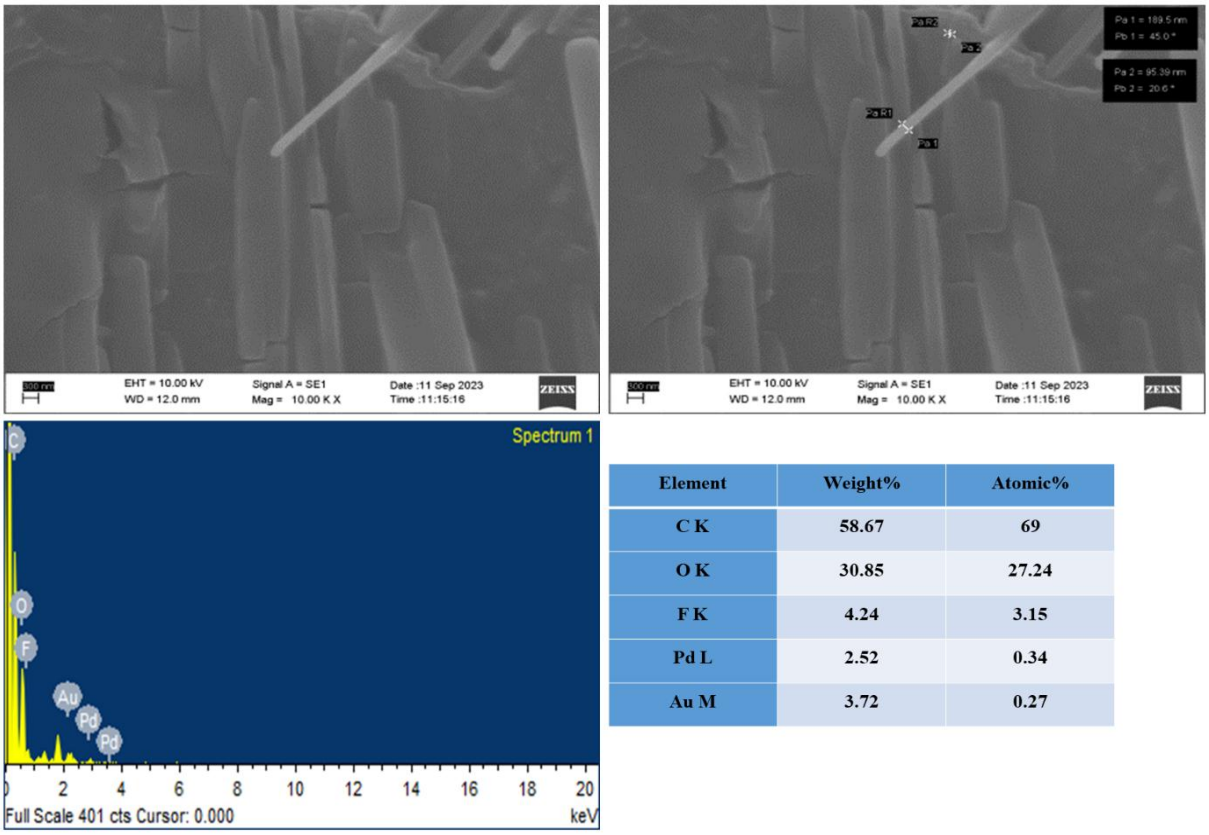

Element	Weight%	Atomic%
C K	58.67	69
O K	30.85	27.24
F K	4.24	3.15
Pd L	2.52	0.34
Au M	3.72	0.27

Figure-4b: SEM and EDX images of Fluconazole Nanoparticles.

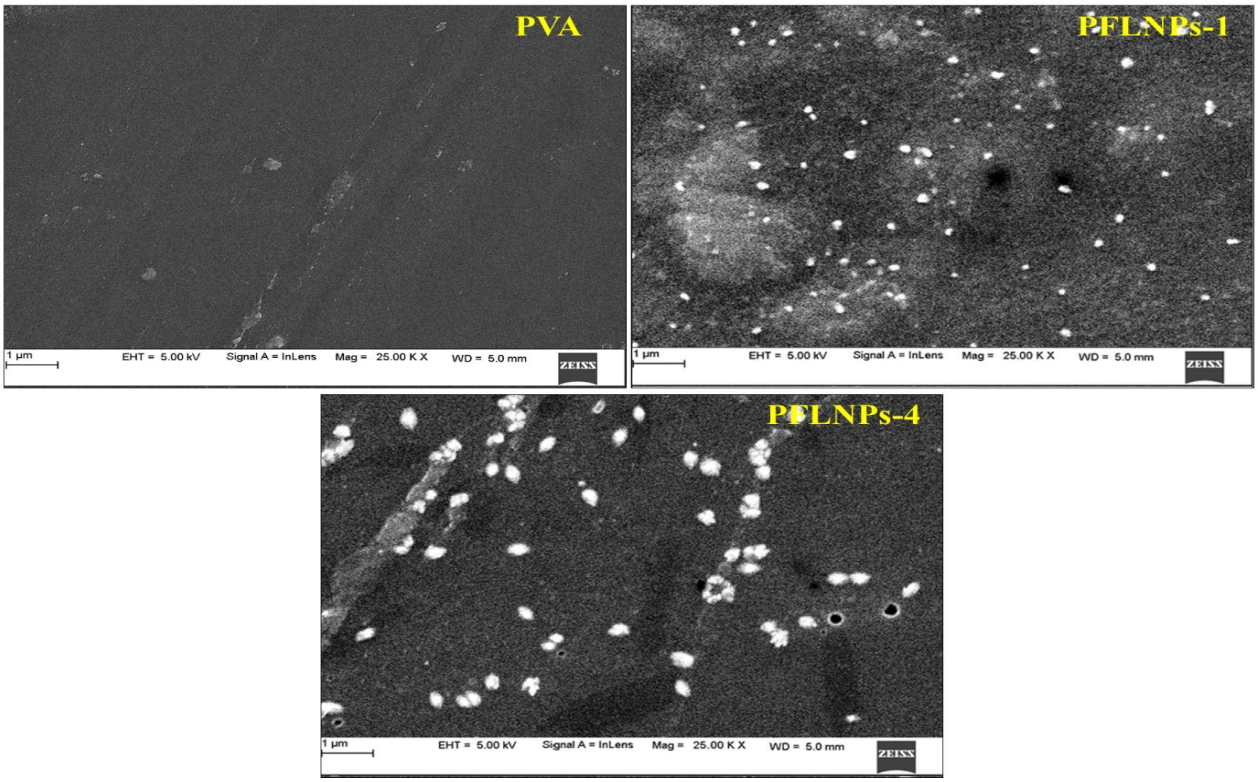

Figure-5: SEM micrographs of pure PVA and PFLNPs composite films.

Mechanical studies: In order to determine the effect that nanoparticles have on mechanical parameters such as tensile strength, Young's modulus, and elongation at break, the films that were created were subjected to mechanical testing, and the results were compiled in Table-2. To enhance the understanding of mechanical performance, stress-strain curves are exhibited in Fig.6 The findings of the mechanical properties showed a notably elevated value. The integration of nanoparticles into the PVA has demonstrated an enhancement in tensile strength (Ts) when compared to pure PVA. It is possible that an increase in the concentration of nanoparticles has been observed in relation to Ts.Furthermore, the incorporation of nanoparticles also affects Young's modulus and percentage elongation at break. Young's modulus increases with higher concentrations of nanoparticles, while elongation at break significantly decreases. This may be assigned to the strong interaction and dispersibility of nanoparticles in the PVA. The stress–strain curves presented in Fig.6 demonstrate that the pure PVA film exhibits flexibility and elasticity, while the nanoparticles doped PVA films show a decrease in elongation and flexibility. For the PFLNPs-1 to PFLNPs-4 series, it is observed that the films exhibit increased brittleness and rigidity, alongside a decrease in flexibility, as the concentration of nanoparticles rises.

Water contact angle measurement: In order to get an understanding of the surface wettability, the nanocomposite films made of PVA and PFLNPs that had been manufactured were examined using a water contact angle analyzer by employing the sessile drop application technique. The contact angle measurements for the PVA and PFLNPs composite films after they have been cleaned and immaculate are shown in Figure 7. The contact angle of 62.87° indicates that pure PVA film exhibits a hydrophilic nature. Significant changes in the contact angle of PFLNPs composite films have been observed. The prepared PFLNPs composite films demonstrated a slight increase in contact angle, measuring 71.12° for PFLNPs-1, 75.08° for PFLNPs-2, and 76.58° for PFLNPs-4. The fact that this is the case shows that the incorporation of FLNPs into the PVA film leads to a decrease in the hydrophilic properties of the PVA film in contrast to the PVA films that have not been changed. The films had a certain degree of hydrophobicity, as seen by the increasing contact angle, which suggests a tendency towards stronger hydrophobic properties. The reduction in hydrophilicity observed may be attributed to the interaction of nanocomposite surfaces with a diminished number of hydroxyl moieties, which potentially accounts for the increased water contact angle noted in the presence of PFLNPs within the PVA matrix. Composite films could gain advantages from the hydrophilic characteristics of PFLNPs, as these properties facilitate the cross-linking of congeners and minimize empty spaces within the matrix, ultimately leading to a decrease in polymer chain mobility. As a result of the increased surface roughness, the wetting liquid's capacity to interact with and permeate the surface of the nanocomposite is restricted[31]. This is because the surface roughness has risen.

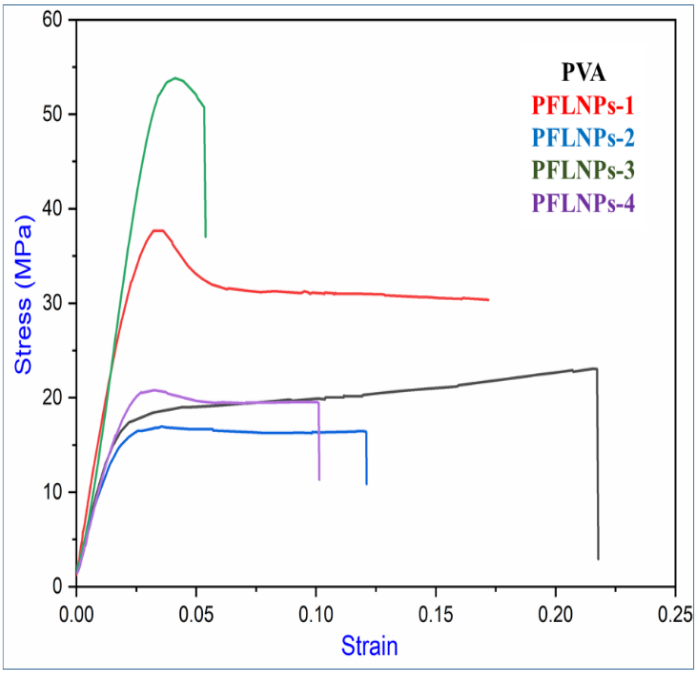

Figure-6: Stress-strain curve of pure PVA and FLNPs composite films.

Table-2: Mechanical properties of PVA and FLNPs composite films.

Sample Code	Thickness of the film (micro meters)	Tensile Strength (Ts)	Youmg;s Modulus (Ym)	% of Elongation at Break
PVA	0.0867	28.25	16.21	187.25
PFLNPs-1	0.0975	69.84	1883.30	15.41
PFLNPs-2	0.1032	64.17	2524.54	13.33
PFLNPs-3	0.1038	66.71	3719.84	11.95
PFLNPs-4	0.1041	64.04	2600.63	6.70

Antimicrobial studies: The agar well diffusion technique was used in order to assess the effectiveness of the nano composite films as antibacterial agents against two gram-positive bacteria and two gram-negative bacteria. Through a series of photos, Figure-8 presents an illustration of the antibacterial action. There is a correlation between the width of the zone of inhibition that surrounds the wells and the antibacterial activity of the biofilms that are shown in Table-3. It was found that the inhibition zones ranged in size from 10 to 26 millimeters across all of the species that were investigated.The highest zone of inhibition was noted in the gram-positive bacterium *S. aureus*, while *B. cereus* showed moderate susceptibility to PVA and PFLNPs-2 composite films. Among the Gram-negative bacteria, *E. coli* exhibited no inhibition against any of the polymers tested. P. aeruginosa demonstrated a moderate level of susceptibility to all polymers. The study of antimicrobial activity showed that the nanocomposite of fluconazole and PVA is more effective at killing bacteria than pure PVA. PFLNPs nanocomposite is a good way to package food because it has a high surface area-to-volume ratio, can be shaped and changed chemically, and can interact with biomolecules to make absorption easier across the cell membrane. These are the main benefits of using PFLNPs nanocomposite as a food packing system. Also, the protein-fluconazole complex is better at interacting with different transport proteins in the body than the PFLNPs nanocomposite-protein complex. The enhanced interaction arises from the presence of two triazole rings alongside two highly electron-withdrawing fluorine atoms found in fluconazole[32]. It can be inferred that the PFLNPs composite films have potential applications in food packaging and biomedical fields.

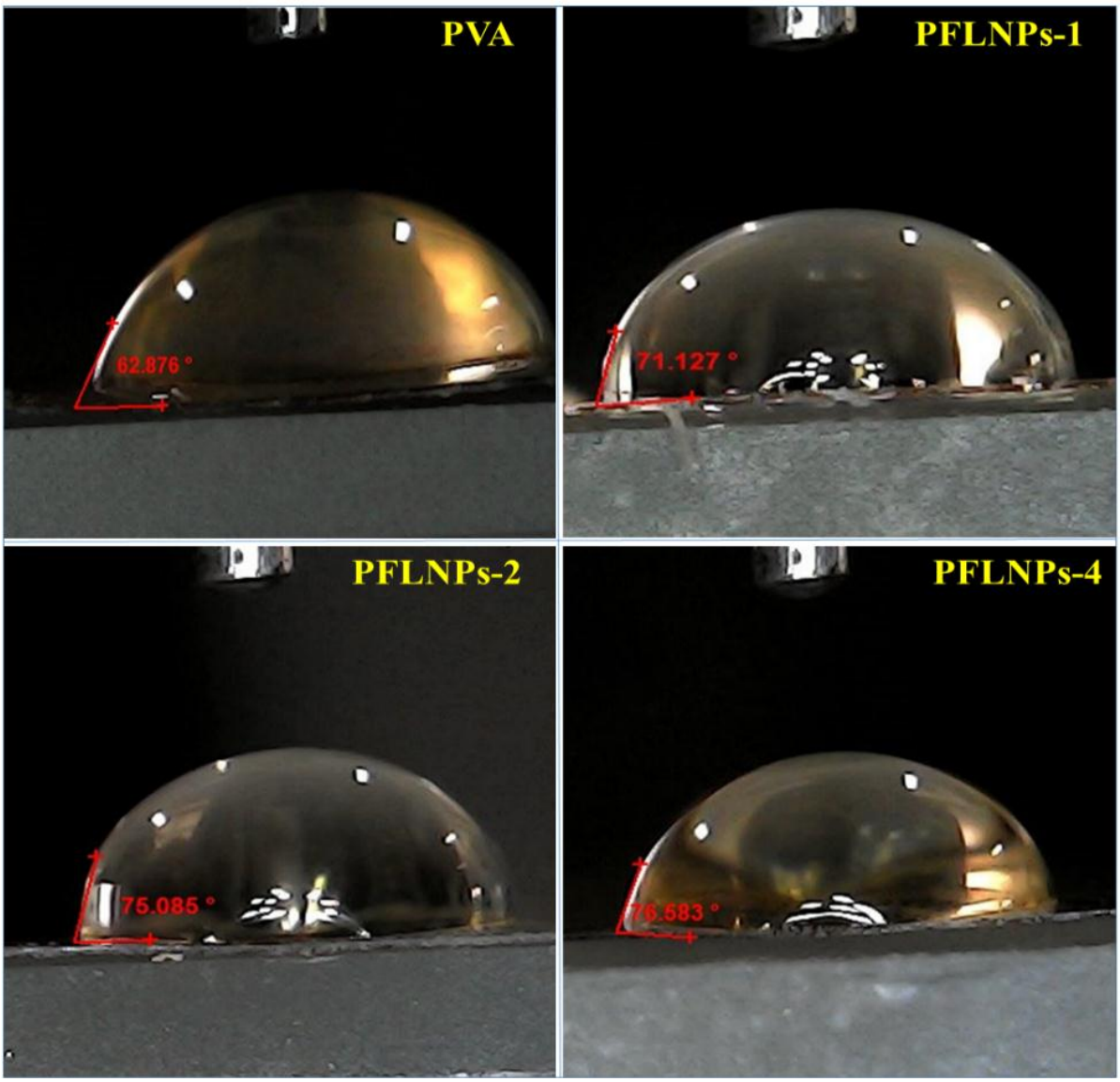

Figure-7: Water contact images of pure PVA and PFLNPs-1, PFLNPs-2 and PFLNPs-4 nanocomposite films.

Table-3: Antimicrobial activity pure PVA and PFLNPs composite films.

Sample	Diameter of Zone of inhibition (mm)			
	Staphylococcus aureus	*Bacillus cereus*	*E.coli*	*P.aeruginosa*
PVA	12	16	00	12
PFLNPs-1	17	12	00	13
PFLNPs-2	14	00	00	14
PFLNPs-3	13	00	00	13
PFLNPs-4	15	00	00	15
Streptomycin (Control)	35	30	27	32

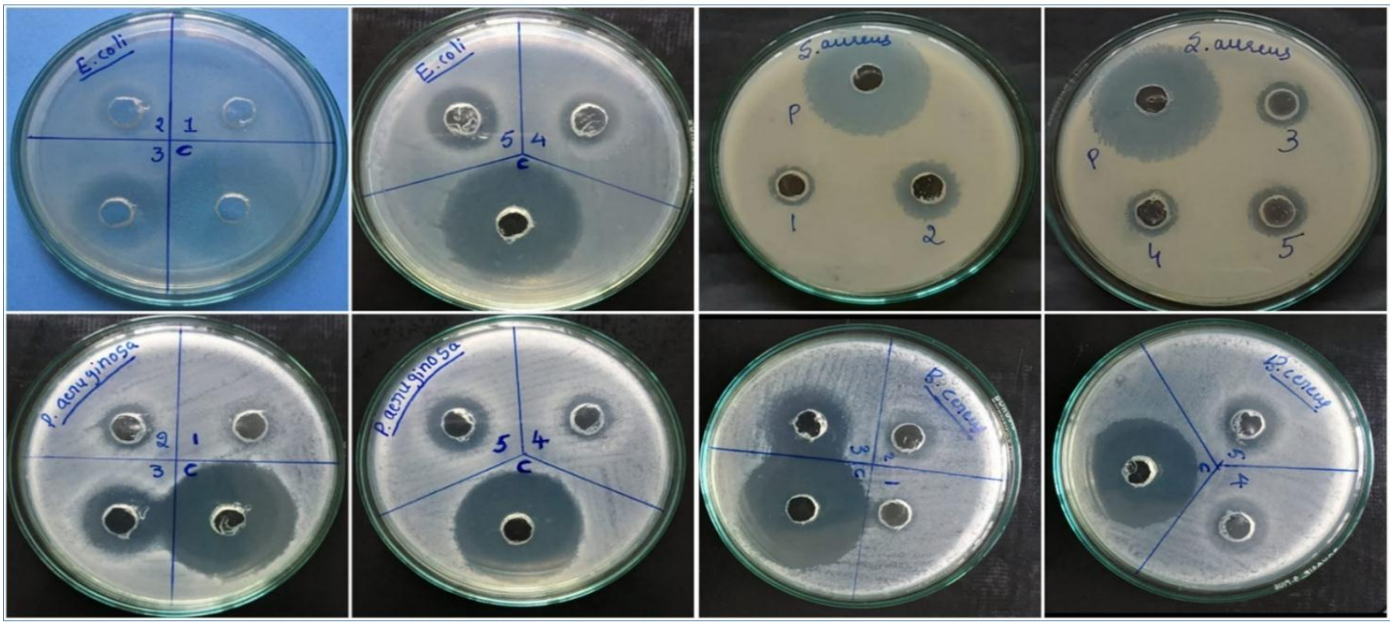

Figure-8: Photographic images of antibacterial activity of nanocomposites (a) Gram +ve bacteria; *S. aurous and B. cereus* (b) Gram negative bacteria; *E. coli and P. aeruginosa*. (Note: C-control, 1-PVA, 2-PFLNPs-1, 3-PFLNPs-2, 4-PFLNPs-3, 5-PFLNPs-4 code mentioned in the images)**.**

Conclusion

The composite films of PVA doped with PFLNPs were effectively prepared using the solvent casting method. The analysis of structural and morphological characteristics was conducted utilizing UV, FT-IR, XRD, SEM, and WCA measurement techniques. The mechanical properties and antimicrobial activities of the prepared PFLNPs composite films were also examined. The structural and morphological analyses confirmed the successful integration of PFLNPs into the PVA film. The detection of a UV absorption peak at 374 nm indicates the successful formation of nanoparticles, while the FTIR spectra reveal the establishment of hydrogen bonds between PVA and PFLNPs, confirming the interaction between the polymer and the dopant. The Water contact angle along with mechanical and antimicrobial analysis, indicated a reduction in hydrophilicity, an enhancement in mechanical properties, and the composite films demonstrated significant antimicrobial activity.The findings suggest that PFLNPs-doped PVA composite films may have promising applications in food packaging. The future scope of this study will encompass an exploration of usability across a diverse array of food packaging and biomedical applications.

Acknowledgements

The authors thank Jain University's engineering and technology faculty. Bangalore, the Department of Chemistry, Karnataka

Science College in Dharwad, and the Department of Studies in Biotechnology and Microbiology at Karnataka University, Dharwad, as well as the DST-PURSE Research Facility Centre at Mangalore University, for their significant support and critical resources, which helped complete this research.

References

1. Amaregouda, Y., Kamanna, K., & Gasti, T. (2022). Biodegradable Polyvinyl Alcohol/Carboxymethyl Cellulose Composite Incorporated with l-Alanine Functionalized MgO Nanoplates: Physico-chemical and Food Packaging Features. *Journal of Inorganic and Organometallic Polymers and Materials*, 32(6), 2040-2055. https://doi:10.1007/s10904-022-02261-9

2. Rodríguez, G. M., Sibaja, J. C., Espitia, P. J. P., & Otoni, C. G. (2020). Antioxidant active packaging based on papaya edible films incorporated with Moringa oleifera and ascorbic acid for food preservation. *Food Hydrocolloids, 103*, 105630. https://doi.org/10.1016/j.foodhyd.2019.105630

3. Gul, W., Akbar Shah, S. R., Khan, A., Ahmad, N., Ahmed, S., Ain, N., Khan, R. (2023). Synthesis of graphene oxide (GO) and reduced graphene oxide (rGO) and their application as nano-fillers to improve the physical and mechanical properties of medium density fiberboard. *Frontiers in Materials*, 10. https://doi:10.3389/fmats.2023.1206918

4. Sarwar, M. S., Niazi, M. B. K., Jahan, Z., Ahmad, T., & Hussain, A. (2018). Preparation and characterization of PVA/nanocellulose/Ag nanocomposite films for antimicrobial food packaging. *Carbohydrate Polymers, 184*, 453-464. https://doi.org/10.1016/j.carbpol.2017.12.068

5. Chiu, I., Ye, H., Aayush, K., & Yang, T. (2024). Intelligent food packaging for smart sensing of food safety. *Adv Food Nutr Res*, 111, 215-259. https://doi:10.1016/bs.afnr.2024.06.006

6. Vajdi, M., Varidi, M. J., Varidi, M., & Mohebbi, M. (2019). Using electronic nose to recognize fish spoilage with an optimum classifier. *Journal of Food Measurement and Characterization*, 13(2), 1205-1217. https://doi:10.1007/s11694-019-00036-4

7. Tawakkal, I. S. M. A., Cran, M. J., & Bigger, S. W. (2016). Interaction and quantification of thymol in active PLA-based materials containing natural fibers. *Journal of Applied Polymer Science*, 133(2). https://doi:https://doi.org/10.1002/app.42160

8. Yousefi, H., Su, H.-M., M. Imani, S., Al-Khaldi, K., Filipe, C., & Didar, T. (2019). Intelligent Food Packaging: A Review of Smart Sensing Technologies for Monitoring Food Quality. *ACS Sensors*, 4. doi:10.1021/acssensors.9b00440

9. Suganthi, S., Vignesh, S., Kalyana Sundar, J., & Raj, V. (2020). Fabrication of PVA polymer films with improved antibacterial activity by fine-tuning via organic acids for food packaging applications. *Applied Water Science*, 10(4), 100. https://doi:10.1007/s13201-020-1162-y

10. Bajer, D., & Burkowska-But, A. (2022). Innovative and environmentally safe composites based on starch modified with dialdehyde starch, caffeine, or ascorbic acid for applications in the food packaging industry. *Food Chemistry, 374*, 131639. :https://doi.org/10.1016/j.foodchem.2021.131639

11. Sarker Ratna, A., Verma, C., Hossain, S., Gupta, B., & Mukhopadhyay, S. (2023). Development of corn husk cellulose reinforced polyvinyl alcohol bio-composite films incorporated with Zinc Oxide nanoparticles. *Bioresource Technology Reports, 23*, 101570. https://doi.org/10.1016/j.biteb.2023.101570

12. Pal, K., Banthia, A. K., & Majumdar, D. K. (2007). Preparation and characterization of polyvinyl alcohol-gelatin hydrogel membranes for biomedical applications. *AAPS Pharm Sci Tech*, 8(1), 21. https://doi:10.1208/pt080121

13. Kumaraswamy, S., & Mallaiah, S. H. (2016). Swelling and mechanical properties of radiation crosslinked Au/PVA hydrogel nanocomposites. *Radiation Effects and Defects in Solids*, 171, 869-878. https://doi:10.1080/10420150.2016.1250095

14. Zhang, Y., Zhu, P. C., & Edgren, D. (2010). Crosslinking reaction of poly(vinyl alcohol) with glyoxal. *Journal of Polymer Research*, 17(5), 725-730. https://doi:10.1007/s10965-009-9362-z

15. Sonker, A. K., Rathore, K., Nagarale, R. K., & Verma, V. (2018). Crosslinking of Polyvinyl Alcohol (PVA) and Effect of Crosslinker Shape (Aliphatic and Aromatic) Thereof. *Journal of Polymers and the Environment*, 26(5), 1782-1794. . https://doi:10.1007/s10924-017-1077-3

16. Carbone, M., Donia, D. T., Sabbatella, G., & Antiochia, R. (2016). Silver nanoparticles in polymeric matrices for fresh food packaging. *Journal of King Saud University - Science, 28*(4), 273-279. https://doi.org/10.1016/ j.jksus.2016.05.004

17. Rhim, J. W., Park, H. M., & Ha, C.-S. (2013). Bio-nanocomposites for food packaging applications. *Progress in Polymer Science*, *38*(10), 1629-1652. https://doi.org/10.1016/j.progpolymsci.2013.05.008

18. Atta, N., Amin, K., El-Rehim, H., & Galal, A. (2015). Graphene prepared by gamma irradiation for corrosion protection of stainless steel 316 in chloride containing electrolytes. *RSC Advances*, 5, 71627-71636. https://doi:10.1039/c5ra11287g

19. Bryaskova, R., Pencheva, D., Kale, G. M., Lad, U., & Kantardjiev, T. (2010). Synthesis, characterisation and

antibacterial activity of PVA/TEOS/Ag-Np hybrid thin films. *J Colloid Interface Sci*, 349(1), 77-85. https://doi:10.1016/j.jcis.2010.04.091

20. Sawant, B., & Khan, T. (2017). Recent advances in delivery of antifungal agents for therapeutic management of candidiasis. *Biomedicine & Pharmacotherapy, 96*, 1478-1490. https://doi.org/10.1016/j.biopha.2017.11.127

21. Hendrawan, H., Khoerunnisa, F., Sonjaya, Y., & Putri, A. (2019). Poly (vinyl alcohol)/glutaraldehyde/ Premna oblongifolia merr extract hydrogel for controlled-release and water absorption application. *IOP Conference Series: Materials Science and Engineering, 509*, 012048. https://doi:10.1088/1757-899X/509/1/012048

22. AL-Kadhemy, M. F. H., Ibrahim, S. A., & Salman, J. A. S. (2020). Studying the physical properties polyvinyl alcohol polymer mixture with silica nanoparticles and its application as pathogenic bacteria inhibitor. *AIP Conference Proceedings, 2290*(1). https://doi:10.1063/5.0028817

23. Dash A K Elmquist W F Wozniak T J Brittain H G Al-Badr A A Kumar K Dash A K Mazzo D J Florey K Shervington L lndrayanto G (2001). San Diego. Academic Press. 67–113. ISBN 13: 9780970077301

24. Morteza-Semnani, K., Saeedi, M., Akbari, J., Moazeni, M., Seraj, H., Tajbakhsh, M., . . . Babaei, A. (2021). Fluconazole Nanosuspension Enhances In Vitro Antifungal Activity against Resistant Strains of Candida albicans. *Pharmaceutical Sciences*, 28. doi:10.34172/PS.2021.21

25. Attia, G., & Abd El-kader, M. (2013). Structural, Optical and Thermal Characterization of PVA/2HEC Polyblend Films. *International Journal of Electrochemical Science, 8*, 5672-5687. https:doi.org/10.1007//s10904-022-02261-9

26. Gupta, S., Pramanik, A. K., Kailath, A., Mishra, T., Guha, A., Nayar, S., & Sinha, A. (2009). Composition dependent structural modulations in transparent poly(vinyl alcohol) hydrogels. *Colloids and Surfaces B: Biointerfaces, 74*(1), 186-190. https://doi.org/10.1016/j.colsurfb.2009.07.015

27. Abdelaziz, M., & Abdelrazek, E. M. (2007). Effect of dopant mixture on structural, optical and electron spin resonance properties of polyvinyl alcohol. *Physica B: Condensed Matter, 390*(1), 1-9. https://doi.org/10.1016/j.physb.2006.07.067

28. Li, Y., Luan, Y., Liu, W., Wang, C., Cao, H., & Liu, P. (2022). Cellulose nanofibrils/polyvinyl alcohol/silver nanoparticles composite hydrogel: Preparation and its catalyst degradation performance of cationic dye. *Journal of Applied Polymer Science*, 139(22), 52246. https://doi.org/10.1002/app.52246

29. Mokhtari-Hosseini, Z.-B., Hatamian-Zarmi, A., Mahdizadeh, S., Ebrahimi-Hosseinzadeh, B., Alvandi, H., & Kianirad, S. (2022). Environmentally-Friendly Synthesis of Ag Nanoparticles by Fusarium sporotrichioides for the Production of PVA/Bentonite/Ag Composite Nanofibers. *Journal of Polymers and the Environment*, 30(10), 4146-4156. https://doi:10.1007/s 10924-022-02509-y

30. Hernandez Nuñez, E., Martínez-Gutierrez, C., López-Cortés, A., Aguirre-Macedo, M., Tabasco, C., Gonzalez-Díaz, M., & García-Maldonado, J. (2019). Physico-chemical Characterization of Poly(3-Hydroxybutyrate) Produced by Halomonas salina, Isolated from a Hypersaline Microbial Mat. *Journal of Polymers and the Environment, 27*. https://doi:10.1007/s10924-019-01417-y

31. Hasheminya, S.-M., Rezaei Mokarram, R., Ghanbarzadeh, B., Hamishekar, H., & Kafil, H. S. (2018). Physicochemical, mechanical, optical, microstructural and antimicrobial properties of novel kefiran-carboxymethyl cellulose biocomposite films as influenced by copper oxide nanoparticles (CuONPs). *Food Packaging and Shelf Life, 17*, 196-204. https://doi.org/10.1016/j.fpsl.2018.07.003

32. Ghosh, M., Mandal, S., Roy, A., Chakrabarty, S., Chakrabarti, G., & Pradhan, S. K. (2020). Enhanced antifungal activity of fluconazole conjugated with Cu-Ag-ZnO nanocomposite. *Materials Science and Engineering: C, 106*, 110160. https://doi.org/10.1016/j.msec.2019.110160

33. Hoa, L., Tai, N., Nguyen, L., & Dang, C. (2011). Preparation and characterisation of nanoparticles containing ketoprofen and acrylic polymers prepared by emulsion solvent evaporation method. *Journal of Experimental Nanoscience - J Exp Nanosci, 7*, 1-9. https://doi:10.1080/17458080.2010.515247

34. Morteza-Semnani, K., Saeedi, M., Akbari, J., Moazeni, M., Seraj, H., Tajbakhsh, M., . . . Babaei, A. (2021). Fluconazole Nanosuspension Enhances In Vitro Antifungal Activity against Resistant Strains of Candida albicans. *Pharmaceutical Sciences, 28*. https://doi:10.34172/PS.2021.21

35. Agarwal, M., Agarwal, M., Shrivastav, N., Pandey, S., Das, R., & Gaur, P. (2018). Preparation of Chitosan Nanoparticles and their In-vitro Characterization. *International Journal of Life-Sciences Scientific Research*, 4, 1713-1720. https://doi:10.21276/ijlssr.2018.4.2.17.